# Dry desulfurization using MgO by-products: a sustainable alternative

R. del Valle-Zermeño[*,1], J. de Montiano-Redondo[2], J.Formosa[1], J.M. Chimenos[1], M.J. Renedo[2], J. Fernández[2]

1 Departament de Ciència de Materials i Enginyeria Metal·lúrgica, Universitat de Barcelona, Martí I Franquès, 1, E-08028 Barcelona, Spain

2 Departamento de Química e Ingeniería de Procesos y Recursos (QuIPRe), Universidad de Cantabria, Avda. de los Castros s/n, E-39005 Santander, Spain

* Corresponding author: Tel.: +34 93 402 13 16; Fax: +34 93 403 54 38. E-mail address: rdelvallez@ub.edu

## Abstract

Even though Wet Flue Gas Desulfurization (WFGD) has been the most widely applied method for $SO_2$ removal, the great quantity of water needed for the process to take place and the significant amounts of wastewater produced stand out as the main drawbacks. On the other hand, dry desulfurization has attracted much interest because it avoids wastewater managing problems while providing acceptable removal efficiencies. The Industrial Emissions Directive (2010/75/EU) has been demanding the Cement, Lime and Magnesium Oxide industries to reduce their $SO_2$ emissions to limits as low as 50 $mg \cdot Nm^{-3}$ by means of sustainable methods. The authors already reported a WFGD method with a 100% removal efficiency in a closed loop process: the by-products from the calcination process itself were reused as desulfurization agents. In order to further extend the applicability of this kind of by-products and reduce the quantity of water needed, the aim of this study was to assess the desulfurization performance of the same MgO by-products in a dry desulfurization method. These by-products are characterized for being a mixture of mainly magnesium (hydr)oxides and different proportions of calcium (hydr)oxides, dolomite, siliceous materials and other impurities such as Fe and S, altering their alkaline behaviour and therefore their desulfurization potential. Each by-product has been modified by means of hydration in order to increase their desulfurization potential. Thus, the raw and modified by-products have been evaluated in dry desulfurization conditions at low temperature by putting them into contact with a stream of flue gas typical of thermal power plants. Different mass samples were considered and the desulfurization potential of by-products (L of $SO_2$ adsorbed per kg of by-product) was determined and used as an efficiency parameter. The reaction products were subsequently characterized in order to define the role of each alkaline phase during $SO_2$ adsorption and delimitate any route of the reutilization. By this manner, the reuse of these by-products could decrease the cost of the process while enhancing sustainability criteria and recyclability. This is, to the knowledge of the authors, the first closed-loop dry desulfurization study that is considering the use of magnesium-based by-products.

# 1. Introduction

The Industrial Emissions Directive of the European Union (2010/75/EU) has been demanding the cement, lime and magnesium oxide industries to reduce their $SO_2$ emissions to limits as low as 50 $mg \cdot Nm^{-3}$ by means of sustainable methods. Therefore, in the case of the calcination process for obtaining magnesium oxide from natural magnesite, a sustainable wet flue gas desulfurization (WFGD) method with a 100% removal efficiency in a closed loop process was proposed by the authors [1,2]: the by-products from the MgO obtaining were reused as desulfurization agents. Even though WFGD has been the most widely applied method for $SO_2$ removal, the large amounts of wastewater effluents are the main drawback. In this sense, dry desulfurization has been presented as an attractive alternative since it avoids wastewater managing problems and requires less energy inputs and lower operation costs [3,4]. At industrial scale, dry desulfurization relies on the atomization of an alkaline sorbent (mainly CaO-based components) in a reaction chamber upstream of a particulate collection device [4–7]. There are some important issues concerning dry desulfurization: the sorbent and the reaction product utilization [5,7]. The chemical reaction between the sorbent and the $SO_2$ is a gas-solid reaction that strongly depends on diffusion mechanisms and hence on the contact efficiency and contact residence time [8]. In lime-based sorbents, calcium utilization is limited by the precipitation of calcium sulfite formed on the sorbent surface [9]. These issues can be addressed by modifying the CaO particle characteristics, including the surface area, pore size and distribution, and volume [6]. Other enhancing approaches include the improvement of the sorbent's reactivity by blending it with additives, in order to favor the formation of a compound with a larger specific surface area. In this sense, Sanders et al. (1995) early reported that mixing quicklime slurries with coal fly ashes resulted in an enhancement of reactivity due to the formation of a calcium silica hydrate, which possess a high specific surface area [10]. A similar mixture was studied by Hiroaki et al., (1995), where the activity was reported to be closely related to the progress of the hydration reaction and the drying temperature of the hydration products during the preparation procedures [11]. Other similar studies have also aimed at improving hydration conditions of CaO by varying time and temperature [12–14], or by using other additives [9,15,16].
The objectives of developing high-active sorbents for $SO_2$ removal also relay in producing valuable byproducts. Thus, when using CaO-based sorbents, $CaSO_4$ becomes the main reaction product, which makes the process very attractive [8].
Taking into account all the above mentioned, the aim of this study is to assess the desulfurization performance of the by-products from the calcination of natural magnesite in a dry desulfurization process. The dry desulfurization experiments were carried out at low temperatures and using a flue gas with a composition similar to coal-burning kilns. For the effects of comparison, the same by-products from the WFGD studies were taken under consideration [1,2]. In order to improve the reactivity, each by-product was also hydrated by means of a process previously reported by the authors [21]. Thus, the desulfurization results obtained for both the raw and hydrated by-products are herein presented.

# 2. Methods and materials

## 2.1. Raw by-products

Three different kinds of by-products were considered. These by-products were carefully already analysed in a WFGD at laboratory scale [1,20]. Selected samples of around 25

kg each were supplied by Magnesitas Navarras S.A. located in Navarra (Spain). All samples were collected during the calcination process of natural magnesite. Once the magnesite ore is extracted from the natural deposits and selected, it is fed into two rotary kilns at 1200 and 1600°C respectively for calcination. The gases generated from these two kilns are taken to an air pollution control system where fly particles are collected in fabric filters. This dust material is classified as Low-grade MgO (LG-MgO) and was the first by-product considered for study. The second by-product was the corresponding dust material also collected in fabric filters when the natural ore has been enriched in dolomite -$CaMg(CO_3)_2$- and was catalogued as Low-Grade Dolomite (LG-D). At the outlet of the rotary kilns the calcined product is subsequently air quenched and physically classified with respect the particle size. The smaller fraction of caustic calcined magnesia is separated and collected as fine MgO (LG-F), being the third by-product under consideration. All gases used in the dry desulfurization experiments were provided by Air Liquide S.A. The hydration method applied followed the previous experience of the authors [9,21]. It consisted in placing each by-product under stirring (700 rpm) to a 1/4 solid-to-water ratio (S/W) at room temperature for 2 h. The samples were subsequently dried at 110°C for 24 h.

## 2.2. Physicochemical characterization of the by-products

For chemical and physical characterization, a representative subsample (about 5 kg) of each by-product was obtained by quartering each of the initial samples with a riffle-type sample splitter. The three representative subsamples were analysed by X-ray fluorescence (XRF) using a Philips PW2400 X-ray sequential spectrophotometer to elucidate major and minor elements. The crystalline phases were determined by X-ray diffraction (XRD) in a Bragg–Brentano Siemens D-500 powder diffractometer with CuKα radiation. A TA Instruments SDT Q600 Simultaneous TG-DSC was used to perform the thermogravimetic analyses (TGA) in an inert atmosphere of the raw materials (30-1400 °C, 10°C·$min^{-1}$ and a sample mass of approximately 25 mg). Some of the reacted sorbents were analysed by a Setaram thermal analyzer model SETSYS-1700 coupled to a Balzers Thermostar/Omnistro mass spectrometer (30-1350 ºC at 10 ºC·$min^{-1}$ in $N_2$ atmosphere and a sample mass of approximately 10 mg). . The number of m/z signals selected corresponds to $H_2O$ (18), $SO_2$ (64), $SO_3$ (80) and $CO_2$ (44). Acid test was performed in order to evaluate MgO reactivity. The citric acid activity test is designed for determining the reactivity of MgO by acid neutralization using phenolphthalein as indicator. The magnesia activity time is the time elapsed between the addition of acid and the formation of a reddish colour [22]. Acid neutralization values of less than 60 s are used to define highly reactive (soft-burnt) MgO. Medium reactive MgO gives a measure between 180 and 300 s, while a low reactivity MgO (hard-burnt) and a dead-burnt MgO give values greater than 600 s and 900 s respectively [23]. The particle size distribution (PSD) was obtained by using a Beckman Coulter LS 13 320 laser analyzer in polar media to avoid hydration and the specific surface by BET single point method with a Micrometrics Tristar 3000 apparatus.

## 2.3. Desulfurization experiments

The desulfurization experiments were carried out using the laboratory experimental assembly shown in Figure 1. A gas flow of approximately 1000 mL·$min^{-1}$ was mixed and prepared prior entering the desulfurization reactor. The gas mixture containing 785, 120 and 95 mL·$min^{-1}$ of $N_2$, $CO_2$, and synthetic air respectively was humidified to a 55%

of relative humidity before being mixed with 2.5 mL· $min^{-1}$ of $SO_2$ for obtaining the desirable gas composition (12% $CO_2$, 9.5% air, 0.025% $SO_2$ and 78.5% $N_2$).

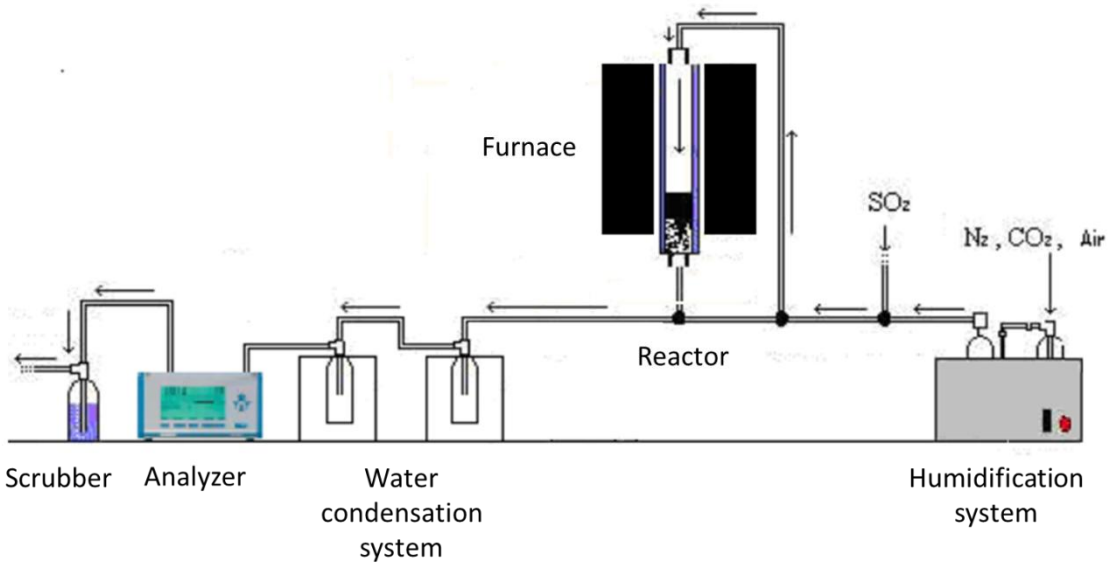


Figure 1. Experimental scheme of the dry desulfurization experiments.

The mix of gases were flowed and humidified until obtaining a stable composition. After humidification and stabilization, the gas mixture was flowed through the reactor (upper inlet) containing each by-product dispersed in inert silica sand (Fontaineblau). This point was considered the start of the experiment. The ratio of by-product to inert silica sand ($B/SiO_2$) varied depending on the amount of sample tested, 1 g of by-product / 30 g silica or 3 g of by-product / 50 g of silica. By this manner, over pressure in the system was avoided. The desulfurization potential of hydrated by-products was also evaluated. Table 1 presents a summary of the experimental trials.

Table 1. Summary of the desulfurization experimental trials

| **By-product** | **Conditions** | **$B/SiO_2$** | |
|---|---|---|---|
| LG-MgO | Raw | 1/30 | 3/50 |
| | Hydrated | 1/30 | |
| LG-D | Raw | 1/30 | 3/50 |
| | Hydrated | 1/30 | |
| LG-F | Raw | 1/30 | 3/50 |
| | Hydrated | 1/30 | |

The time of experiment was 1 hour for all trials. The gas flow at the outlet of the desulfurization reactor was conducted to a water condensation system before being continuously analysed with respect to the concentration of $SO_2$ and $CO_2$ using an Emerson MLT-1 NGA 2000 gas analyser. The data was compiled using NGA win control software. In order to separate them from the inert silica sand, the reaction products were sieved to a particle size below 60 μm and subsequently characterised using XRF and TGA. Each experiment was performed by triplicate and the results are presented as the average.

### 2.4. Desulfurization assessment

The desulfurization potential was assessed by means of two parameters: breakthrough curves and desulfurization potential (L of $SO_2$ per kg of by-product). These two approaches allowed comparing the results obtained in this research to those from previous studies [1,2]. Breakthrough curves were directly obtained from the data recorded by the gas analyser by representing the concentration of $SO_2$ (mL $SO_2 \cdot m^{-3}$; ppmv) at the outlet at a given time ($SO_{2,t}$) as a function of that time (t). The desulfurization potential was calculated by taking into account the data obtained in the breakthrough curves using the Equation 1:

——————— ——— (Eq.1)

where *f* is the flow of gases (1 $L \cdot min^{-1}$), Δt is the incremental time considered in the breakthrough curve (min), and *m* is the mass of sample by-product (kg). Values obtained by means of Eq. 1 are the accumulated values and are represented as a function of t.

## 3. Results

### 3.1. Characterization of the by-products

The main chemical composition obtained by XRF analysis, given as most stable oxides of the elements, for the three by-products is shown in Table 2.

Table 2. Chemical composition determined by XRF analysis, acid test results and physical properties for the three by-products.

| | **LG-MgO (%)** | **LG-D (%)** | **LG-F (%)** |
|---|---|---|---|
| MgO | 68.1 | 41.5 | 78.7 |
| CaO | 8.9 | 22.1 | 9.9 |
| $SO_3$ | 8.1 | 8.3 | 2.1 |
| $Fe_2O_3$ | 2.6 | 3.5 | 2.9 |
| $SiO_2$ | 1.5 | 0.7 | 2.8 |
| $K_2O$ | 1.5 | 0.4 | - |
| LOI | 8.7 | 23.1 | 3.6 |
| Acid test | *Hard-burned* | *Dead-burned* | *Dead-burned* |
| BET ($m^2 \cdot g^{-1}$) | 6.6 | 4.6 | 2.6 |
| $d_{50}$ (μm) | 23.1 | 37.5 | 141.4 |

As it can be seen, magnesium was the main element in the three by-products and the calcium content was also important, especially in LG-D. The results from XRF and XRD (not shown) were used along TGA for determining the chemical composition (including carbonates and hydroxides, which were not identified by XRF). Carbonates and hydroxides can be identified by XRD. Thus, the three techniques were used complementary. Figure 2 shows the TG curves (mass loss (%) vs. temperature) of the three by-products.

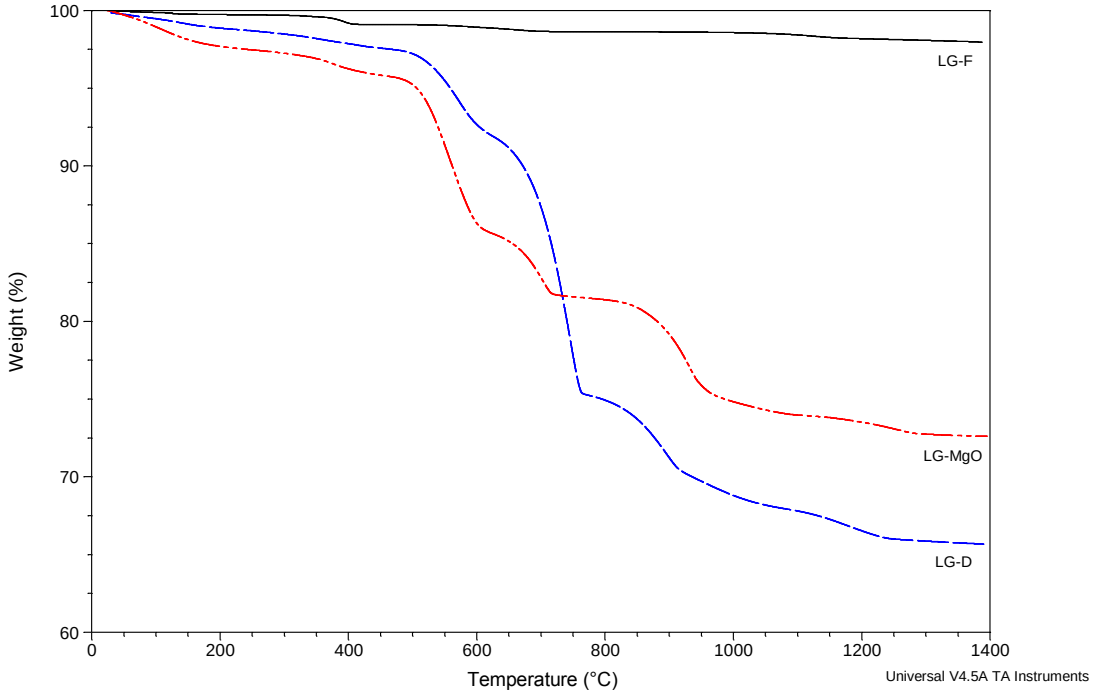


Figure 2. TGA of the raw by-products (LG-MgO, LG-D and LG-F).

The mass loss steps can be generally ascribed to moisture and water of crystallization loss (below 200 ºC), $Mg(OH)_2$ decomposition to MgO releasing $H_2O$ (from 200 to 450 ºC), $MgCO_3$ decomposition to MgO and $CO_2$ (between 450 and 625 ºC), $CaMg(CO_3)_2$ decomposition to MgO, CaO and $CO_2$ (between 625 and 750 ºC), $CaCO_3$ decomposition to CaO and $CO_2$ (up to 1000 ºC), and decomposition of $MgSO_4$ and $CaSO_4$ at around 1100 and 1200 °C respectively. Hence, the mass loss percentages for each reaction of decomposition were used to characterize the carbonates and hydroxides phases of each by-product according to previous studies [21]. The chemical characterization results are presented in Table 3.

Table 3. By-products chemical characterization using XRF, XRD and TGA.

| | LG-MgO (%) | LG-D (%) | LG-F (%) |
|---|---|---|---|
| $Mg(OH)_2$ | 4.2 | 3.9 | 3.4 |
| $MgCO_3$ | 17.2 | 11.1 | - |
| $CaMg(CO_3)_2$ | 6.3 | 33.6 | 1.7 |
| $CaCO_3$ | 15.1 | 10.1 | 0.7 |
| $MgSO_4$ | - | 4.6 | - |
| MgO | 50.1 | 23.5 | 76.7 |
| CaO | - | 5.9 | 8.6 |
| $CaSO_4$ | 1.7 | 3.7 | - |
| Rest | 5.6 | 4.6 | 11.1 |

Magnesium was mainly present as periclase (crystalline MgO) in all by-products, although its presence as uncalcined dolomite was significant in LG-D and to a lesser extent in LG-MgO. The main forms of calcium occurrence were dolomite, calcite, anhydrite, and lime. However, calcium in LG-MgO was only present in the $CaCO_3$ form while in LG-F was presented as CaO. As expected, LG-D presented high amounts of dolomite and a lower content of $CaCO_3$ and $CaSO_4$. The citric acid activity test (see Table 2) showed neutralization times greater than 900 s for both LG-D and LG-F and times greater than 810 for LG-MgO. According to these values, LG-D and LG-F should be termed "dead-burned" magnesia and LG-MgO as "hard-burned" magnesia. It should be noted that this test is defined to categorize highly pure magnesia, therefore the content of CaO in each by-product, as well as the presence of other alkalis, could have also influenced the neutralization of the added acid, resulting in an even higher reactivity. Therefore, it is expected that the reactivity of the magnesia is even lower than that predicted by the citric acid test, as in the case of LG-MgO. Respect to the physical properties (Table 2), LG-MgO and LG-D presented the largest specific surface, calculated using the BET absorption model, 6.6 and 4.6 $m^2 \cdot g^{-1}$ respectively, while LG-F presented 2.6 $m^2 \cdot g^{-1}$. The dust materials (LG-MgO and LG-D) also presented a mean particle size ($d_{50}$) lower than LG-F (23.1, 37.5 and 141.4 µm respectively). Therefore, the by-products differed not only in their chemical compositions but also in their physical characteristics.

## 3.2. Desulfurization Potential

### 3.2.1. Breakthrough curves ($SO_2$ at the outlet vs. time): effect of mass sample

Figures 3, 4 and 5 present the concentration of $SO_2$ at the outlet of the desulfurization reactor as a function of experimental time for raw LG-MgO, LG-D and LG-F respectively. The two mass samples under consideration (1 and 3 g) are included in the figures.

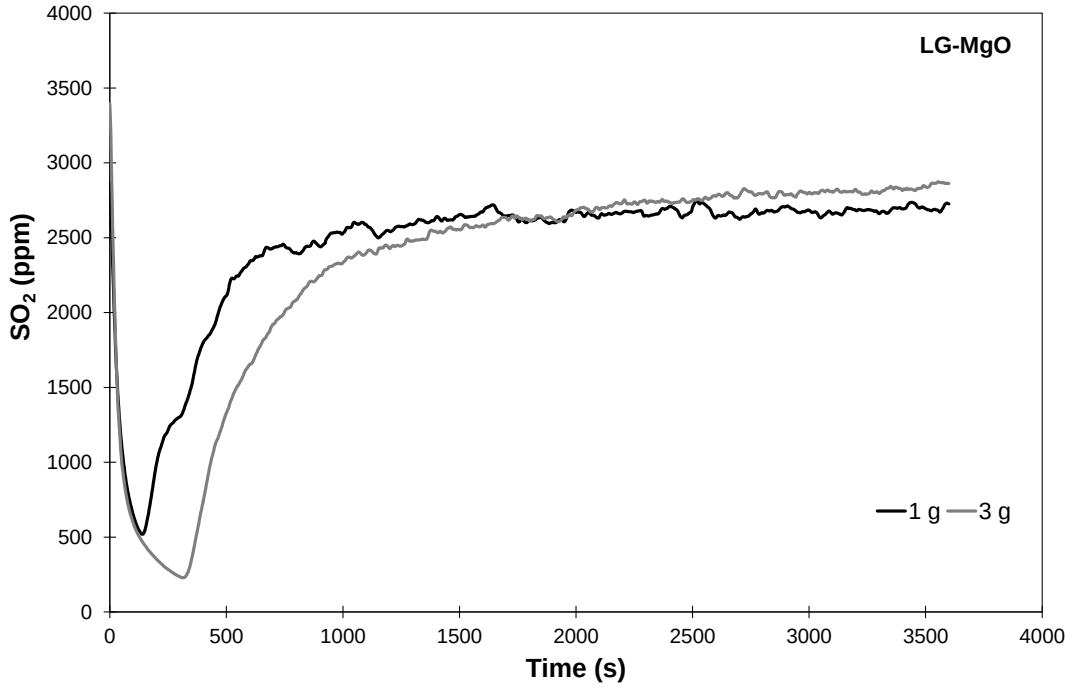


Figure 3. Concentration of $SO_2$ at the outlet (ppm) as a function of time (s) for raw LG-MgO. Effect of mass sample.

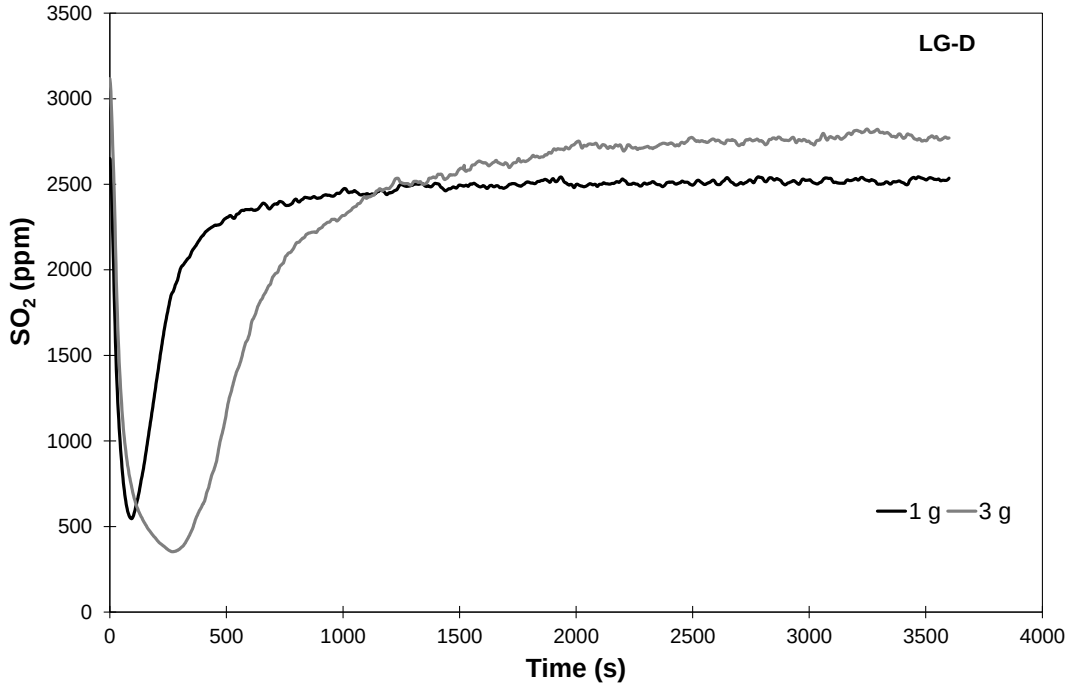


Figure 4. Concentration of $SO_2$ at the outlet (ppm) as a function of time (s) for raw LG-D. Effect of mass sample.

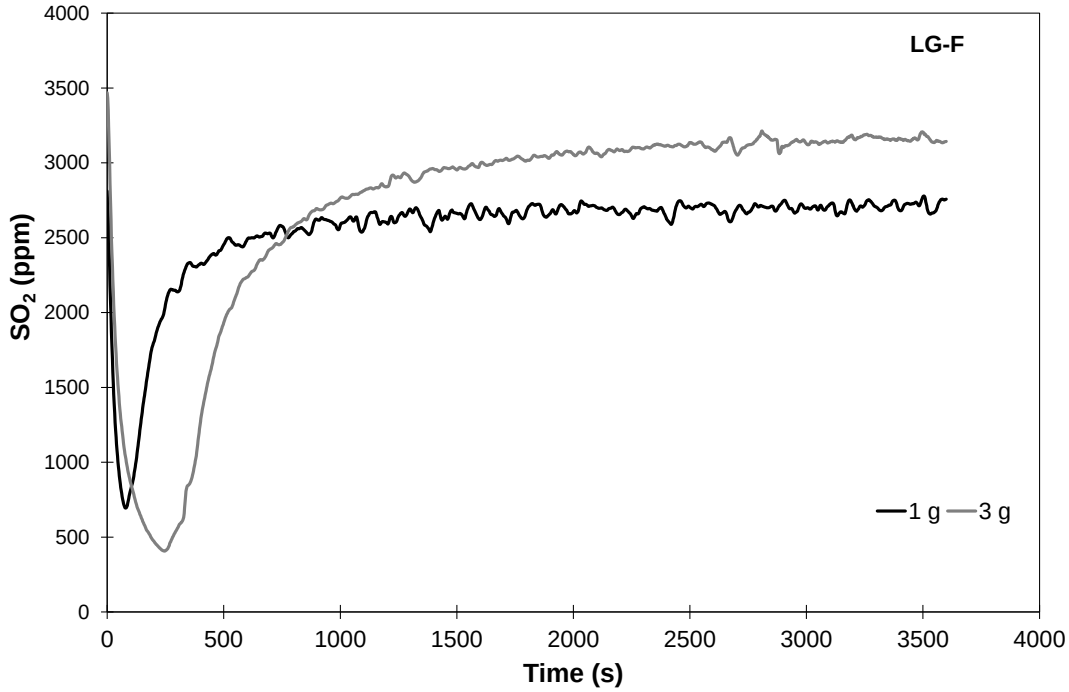


Figure 5. Concentration of $SO_2$ at the outlet (ppm) as a function of time (s) for raw LG-F. Effect of mass sample

As expected, a greater amount of by-product increased the $SO_2$ capture. Breakthrough curves were characterized by a steep controlled by the surface reaction rate followed by a gradual decrease in adsorption. Thus, surface reaction rate dominated initially before diffusion resistance became the limiting step as the generation of the product layer gradually increased**.** Therefore, the chemical reaction rate is important initially, while the product layer diffusion controls the reaction in the end [26].

### 3.2.2. $SO_2$ adsorbed per mass of by-product ($L \cdot kg^{-1}$)

In order to compare the performance among each raw by-product (LG-MgO, LG-D and LG-F), Figures 6 and 7 present the volume of $SO_2$ adsorbed per mass of by-product for 1 and 3 g respectively.

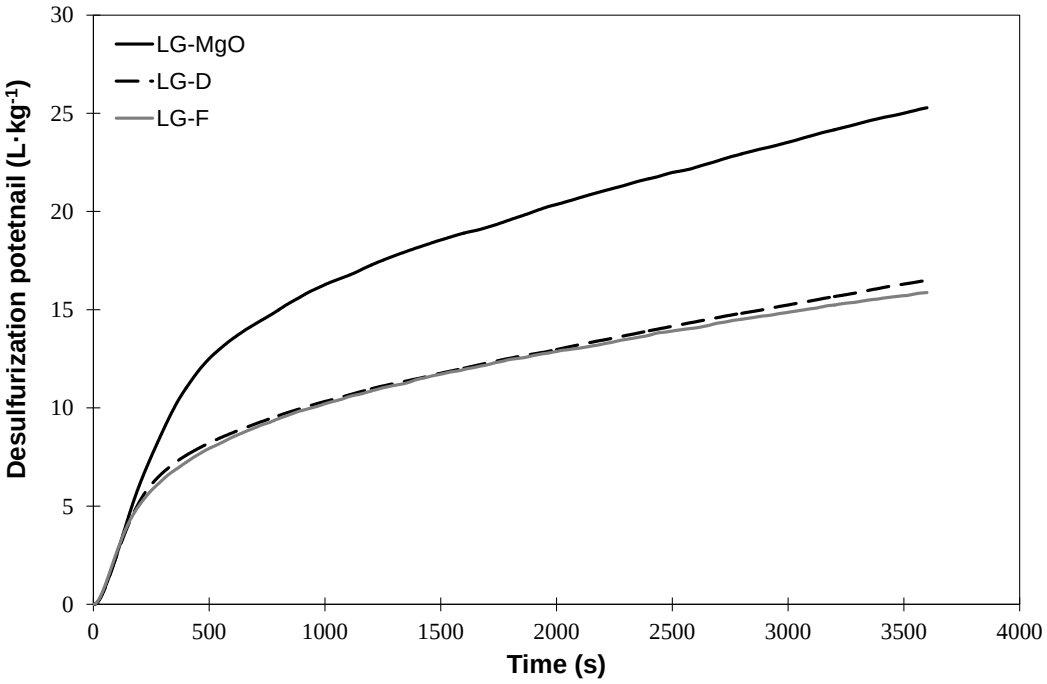


Figure 6. Desulfurization potential (volume of $SO_2$ absorbed per mass of by-product) of 1 g of each of the by-products ($L \cdot kg^{-1}$).

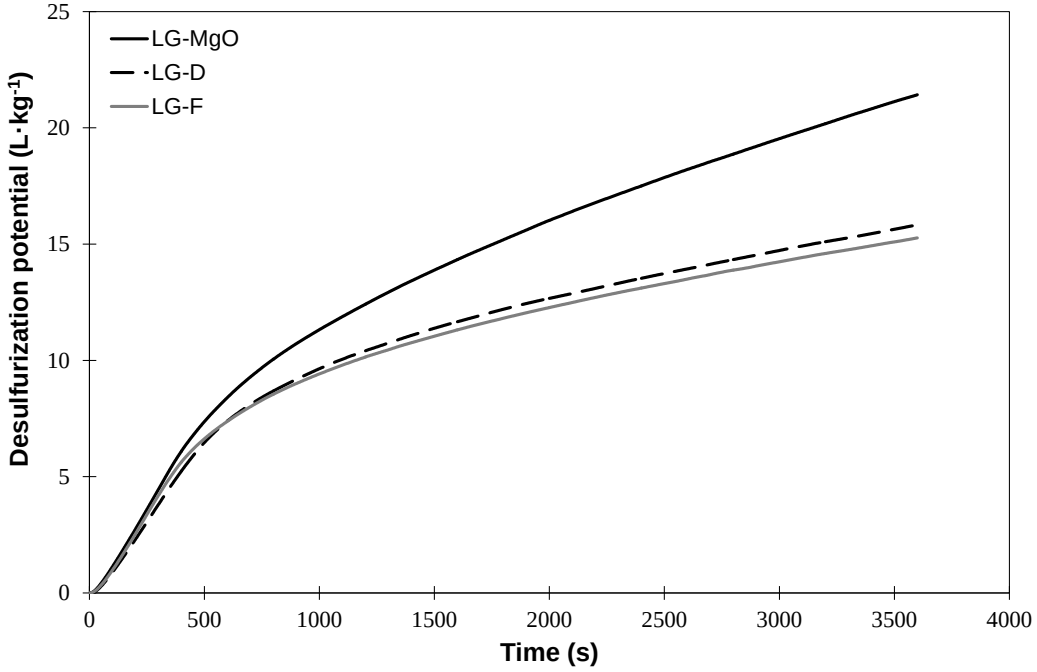


Figure 7. Desulfurization potential (volume of $SO_2$ absorbed per mass of by-product) of 3 g of each of the by-products ($L \cdot kg^{-1}$).

As it can be seen in Figure 4, LG-MgO presented the best sorption capacity, up to 25.2 L of $SO_2$ per kg of by-product. Taking into account that commercial calcium hydroxide with a purity of 89%, tested at these conditions, has a sorption capacity of approximately 50 L of $SO_2$ per kg, the by-product showed a good performance with respect the widely used lime, as in WFGD [1,2,27]. The adsorption capacity of LG-D and LG-F was lower, achieving 16.5 and 15.9 $L \cdot kg^{-1}$ respectively. The amount of by-

product had no significant effect on the adsorption capacity as the values obtained were 21.4, 15.8 and 15.3 $L \cdot kg^{-1}$ for LG-MgO, LG-D, and LG-F respectively (Figure 5). The slightly higher $SO_2$ capture for 1 g of by-product can be attributed to a lower diffusional influence. As Figures show, all samples presented a gradual reduction of the sorption rate as desulfurization proceeded in agreement with the stated in section 3.2.1. The straight line section in all the curves presented in Figure 4 and 5 (for times < 500 s) described the surface reaction control mechanism while the curves tending to stabilization where characteristic of the diffusion created by the layers of reaction products. The greater specific surface area, the higher $Mg(OH)_2$ content and lower particle size of LG-MgO were observed to be not of significant influence on the surface reaction control period. However, the high content of CaO in both LG-D and LG-F raw materials and the fast formation of product covering the particle surface can explain the great difference during the diffusive control period.

### 3.2.3. Effect of hydration

A comparison of the desulfurization potential of each by-product modified by the hydration method is presented in Figures 8, 9, and 10 for LG-MgO, LG-D, and LG-F respectively. The corresponding results of the raw materials (1 g of solid) are included for the sake of comparison.

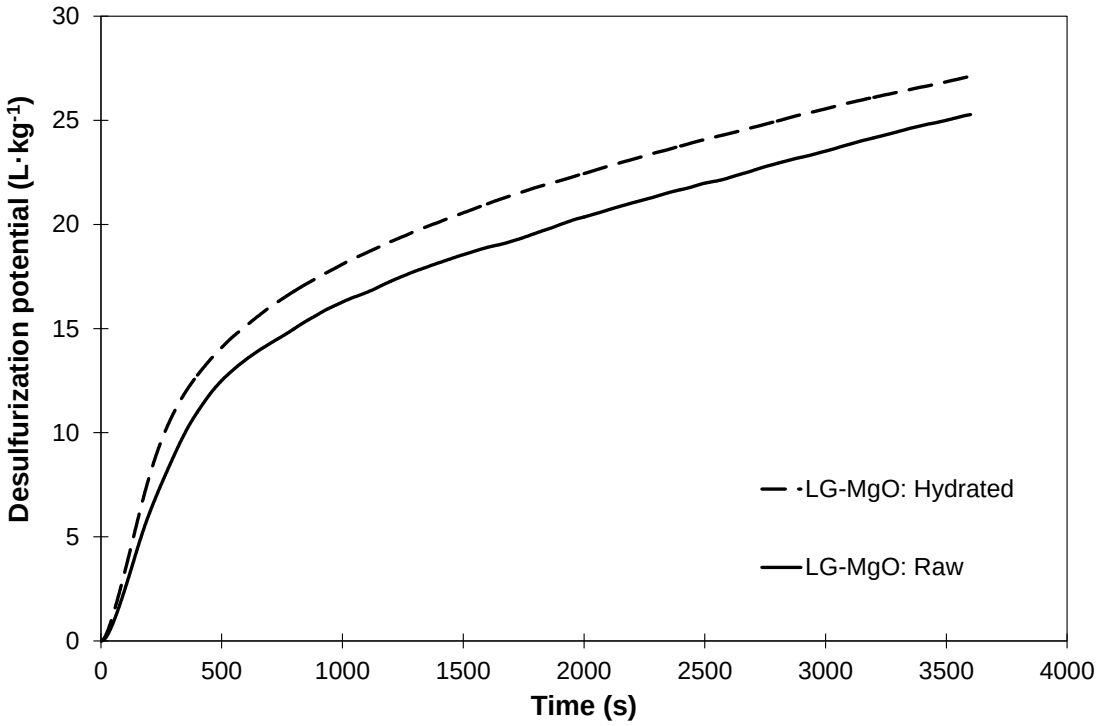


Figure 8. Desulfurization potential ($L \cdot kg^{-1}$) of raw and hydrated LG-MgO.

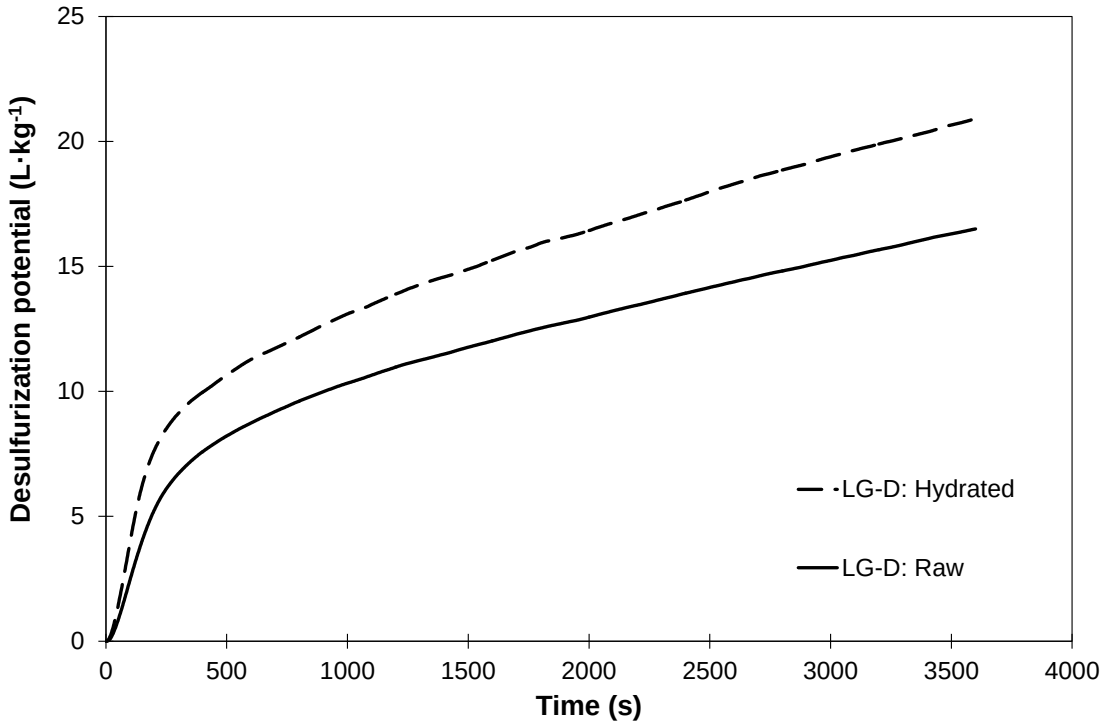


Figure 9. Desulfurization potential ($L \cdot kg^{-1}$) of raw and hydrated LG-D.

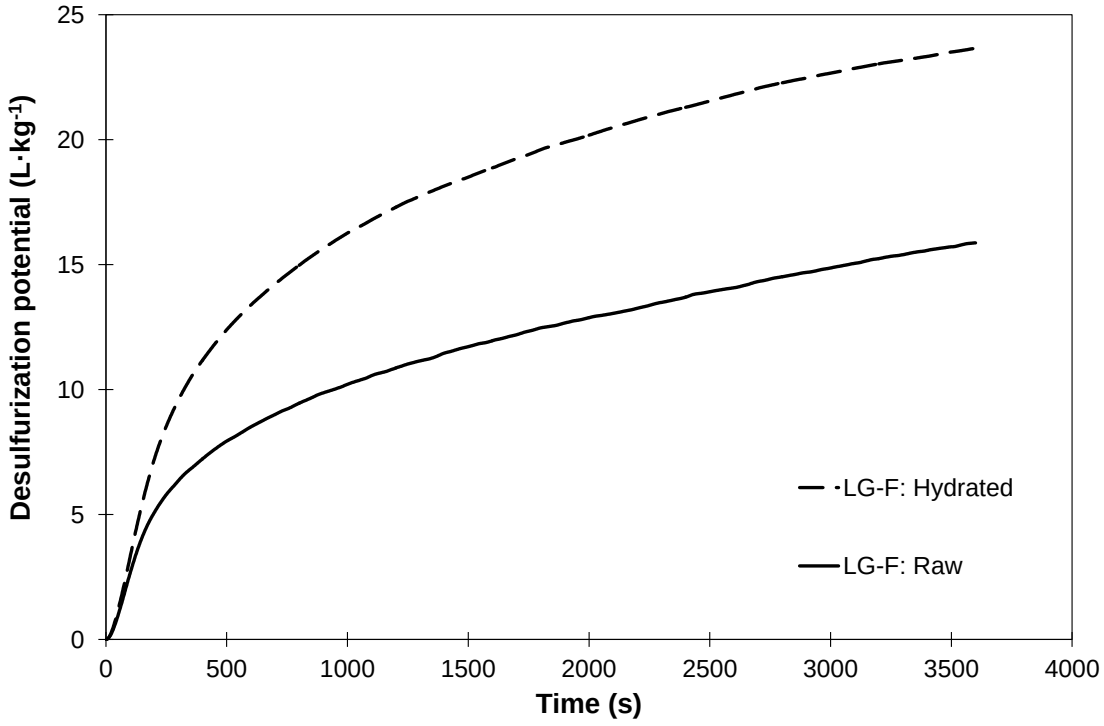


Figure 10. Desulfurization potential ($L \cdot kg^{-1}$) of raw and hydrated LG-F.

As it can be seen, hydration significantly improved the adsorption capacity although each by-product presented a different increase on the sorption enhancement. Hydrated LG-MgO (Figure 8) presented the highest adsorption capacity (27.1 $L \cdot kg^{-1}$), slightly higher than hydrated LG-D and LG-F (20.8 and 23.6 $L \cdot kg^{-1}$ respectively). The improvement in $SO_2$ sorption is attributed to the $Mg(OH)_2$ formed in the hydration (Reaction 1)[28]:

(1)

According to the chemical characterization of the by-products (Table 2), LG-MgO presented 50 % of MgO that to some extent is available to be hydrated. Hydration had a similar effect on LG-D sorption capacity because of the hydration of Ca phases. LG-F, though it contained 76.7 wt% of MgO, was obtained at the end of the calcination kiln and therefore was likely to be partially sintered (see Table 2: lowest BET value, larger $d_{50}$ and catalogued as dead-burnt) [20].

### 3.2.4. Characteristics of the spent sorbents

The XRF analysis of the spent sorbents showed that all samples presented $SiO_2$ content in the 30-40% range, due to an incomplete sieving of the reacted samples. This fact influenced thermal behaviour and the interpretation of the mass loss steps since silica remained unaltered during TGA. Taking this into account, the spent sorbents were analysed qualitatively in order to elucidate the desulfurization mechanism and propose a further potential reutilization of the reaction products formed. According to XRF and XRD, the main reaction products were $MgSO_3$ and $MgSO_4$. The formation of $CaSO_4$ and $CaSO_3$ was limited by the availability of Ca in each by-product. Calcium was partially presented in LG-D and LG-F as CaO and its reaction with water vapour to form $Ca(OH)_2$ prior sulfation was considered the desulfurization route. However, calcium was only present as $CaCO_3$ in LG-MgO. Thus, in order to elucidate the desulfurization route of calcium in LG-MgO, Figure 10a and 10b present the TG-MS results of raw LG-MgO (3 g) after desulfurization in $N_2$ and air atmosphere respectively. The mass loss steps (TG signal, left-y axis) in Figure 10a can be ascribed as water loss (< 200°C), $Mg(OH)_2$ dehydroxilation (350-500°C), $CO_2$ release from $MgCO_3$ decomposition (500-650°C), $CO_2$ release from $CaMg(CO_3)_2$ decomposition (600-900°C) and decarbonation of $CaCO_3$ (900-1000 °C). Along with the mass loss steps, the MS signal (63.96/A) shows a $SO_2$ release at 400ºC and 950ºC. The former can be attributed to the petcoke pyrolysis, which is used as fuel for calcination, as explained by Formosa et al. (2012) [30]. As for the latter, its release was attributed to the decomposition of an alkaline sulphite. The identification of this alkaline sulphite was confirmed by means of Figure 10b, where all the mass loss steps before 900ºC could be described as in Figure 10a. However, in air, the mass loss step attributed to the decomposition of calcite was not detected and a mass loss step at 1300ºC with $SO_2$ release (63.96/A) was observed instead (decomposition of calcium sulphate). Therefore, calcium sulphite was the only reaction product obtained by the reaction of all the calcium carbonate and $SO_2$. Taking this into account, the limestone contained in LG-MgO acted as desulfurization agent along with the MgO phases. In this aspect, previous works reported by the authors allowed to describe the direct sulfation of limestone [27,31]. In that work, the $CaCO_3$ content that remained after the desulfurization reaction with calcium hydroxide was a balance between the $CaCO_3$ present in the raw sorbent, the $CaCO_3$ formed by reaction of calcium hydroxide and $CO_2$ and the $CaCO_3$ that disappeared after reacting with $SO_2$. Therefore, the $CaCO_3$ contained in LG-MgO reacted with $SO_2$ to form calcium sulphite. Accordingly, given the chemical

composition of the reaction products obtained after the desulfurization, these could be further recovered or reutilized, as the $MgSO_4$ contained could be reused for regenerating the sorbent or as fertilizer [28].

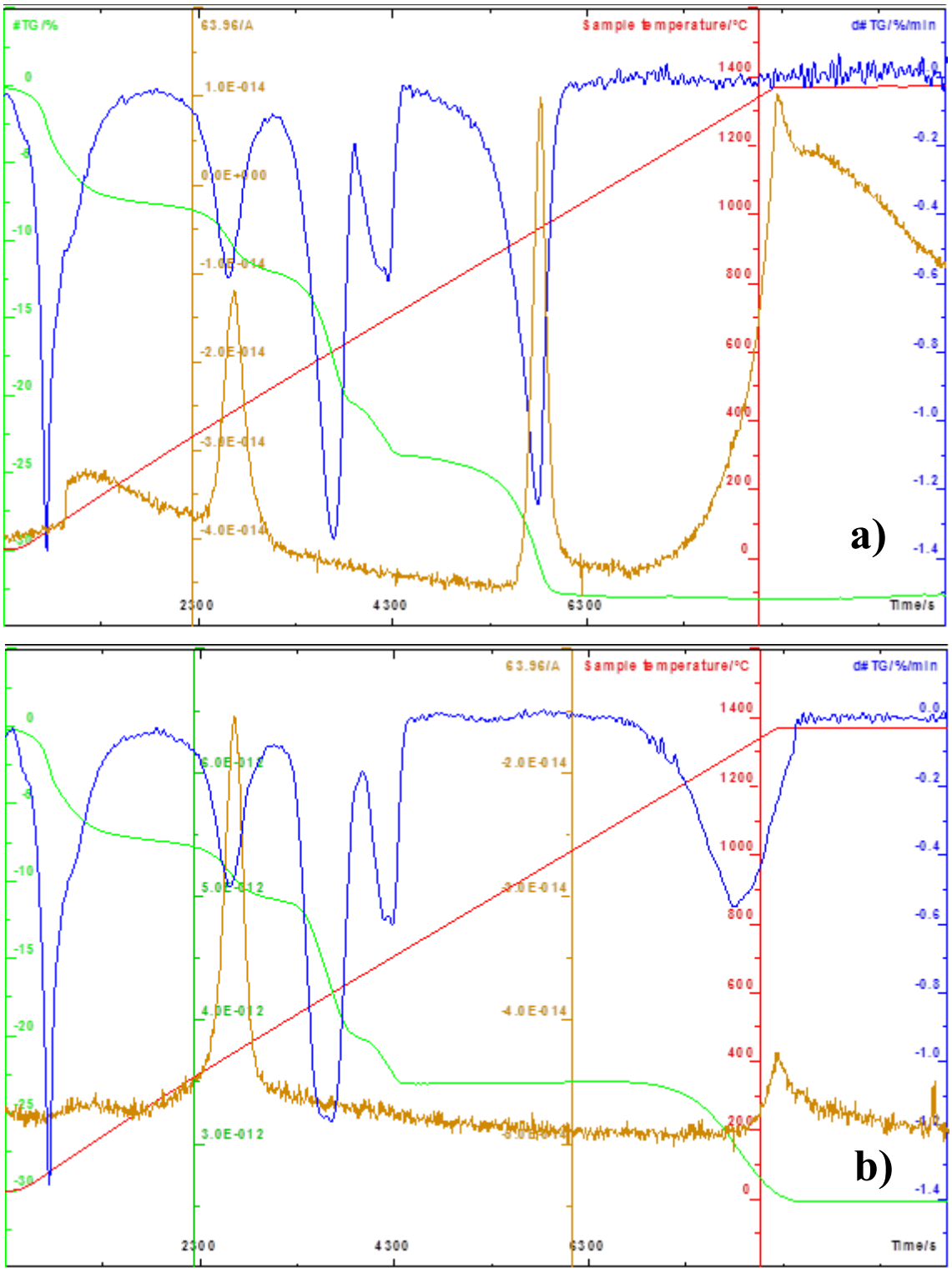


Figure 10. TG, DTG and MS curve ($M^+$ 64, corresponding to $SO_2$) of raw LG-MgO after desulfurization using $N_2$ as the carrier gas (10a) and synthetic air (10b).

### 3.2.5. Comparison with WFGD performance

The average desulfurization potential (L of $SO_2$ per kg) of LG-MgO, LG-D and LG-F for a 100% removal efficiency in a WFGD process were reported to be in the 344-256 $L \cdot kg^{-1}$ range (2.9-3.9 $kg \cdot m^{-3}$) [1,2]. In the same study, the authors compared the by-products performance with that of the widely used lime (834 $L \cdot kg^{-1}$ or 1.2 $kg \cdot m^{-3}$). Therefore, the use of these by-products in a wet process is significantly more effective at totally neutralizing $SO_2$. However, a dry desulfurization process avoids generating wastewater effluents and allows obtaining a solid mixture basically made of $MgSO_3/MgSO_4$ and $CaSO_3/CaSO_4$. Therefore, the compromise between efficiency, consumption of by-product and generation of reaction products has to be analysed and taken into consideration before extrapolating to the industry.

## 4. Conclusions

As an alternative to WFGD, a sustainable dry desulfurization process was studied by assessing the performance of the by-products obtained during the calcination process of natural magnesite. Thus, the by-products from the calcination process that is producing the $SO_2$ emissions could be used as desulfurization agents in a closed-loop process. The three by-products under consideration, LG-MgO and LG-D (dust materials from fabric filters) and LG-F (coarse fraction of the final magnesia product) presented different chemical and physical characteristics. In order to improve the by-products reactivity towards $SO_2$, a hydration method was also applied to the raw by-products. Raw LG-MgO (68.1 wt.%) presented the best desulfurization potential (L of $SO_2$ per kg of by-product), up to 25 $L \cdot kg^{-1}$, very convenient compared to the performance of the widely used lime in the same conditions (50 $L \cdot kg^{-1}$). The adsorption capacity of LG-D and LG-F was lower, achieving 16.5 and 15.9 $L \cdot kg^{-1}$ respectively. The analysis of desulfurization curves (accumulative $L \cdot kg^{-1}$ vs. time) showed that the greater specific surface area, the higher $Mg(OH)_2$ content and lower particle size of LG-MgO were not of significant influence on the surface reaction control period. However, the high content of CaO in both LG-D and LG-F raw materials and the fast formation of product covering the particle surface influenced their behaviour in the diffusive control period. Hydrating the raw by-products allowed to increase the $SO_2$ sorption capacity to up to 27.1 $L \cdot kg^{-1}$ (LG-MgO). The use of the same by-products in a wet process was reported to be more effective than the performance in dry state. However, dry desulfurization avoids generating wastewater effluents while obtaining a solid mixture basically made of $MgSO_3/MgSO_4$ and $CaSO_3/CaSO_4$. These solids could be reused for other applications, allowing further extending the sustainability criteria of the overall process.

## Acknowledgements

The authors would like to thank Magnesitas Navarras S.A for their financial support. Ricardo del Valle Zermeño is grateful to the Government of Catalonia (Departament d'Universitats, Recerca i Societat de la Informació) for the research grant (FI-DGR 2014) and to the Fundació Montcelimar (Barcelona, Spain) for funding.

## References

[1] R. Del Valle-Zermeño, J. Formosa, J.A. Aparicio, J.M. Chimenos, Reutilization of low-grade magnesium oxides for flue gas desulfurization during calcination of natural magnesite: A closed-loop process, Chem. Eng. J. 254 (2014) 63–72.

[2] R. del Valle-Zermeño, M. Niubó, J. Formosa, M. Guembe, J.A. Aparicio, J.M. Chimenos, Synergistic effect of the parameters affecting wet flue gas desulfurization using magnesium oxides by-products, Chem. Eng. J. 262 (2015) 268–277.

[3] Y. Mathieu, L. Tzanis, M. Soulard, J. Patarin, M. Vierling, M. Molière, Adsorption of SOx by oxide materials: A review, Fuel Process. Technol. 114 (2013) 81–100.

[4] F. Scala, M. D'Ascenzo, A. Lancia, Modeling flue gas desulfurization by spray-dry absorption, Sep. Purif. Technol. 34 (2004) 143–153.

[5] P.S. Nolan. Flue Gas Desulfurization Technologies for Coal-Fired Power Plants, The Babcock & Wilcox Company U.S., in: Coal-Tech 200 International Conference, November, 2000, Jakarta, Indonesia.

[6] Y. Li, M. Nishioka, M. Sadakata, High Calcium Utilization and Gypsum Formation for Dry Desulfurization Process, 34 (1999) 1015–1020.

[7] Y. Li, M. Sadakata, Study of gypsum formation for appropriate dry desulfurization process of flue gas, Fuel. 78 (1999) 1089–1095.

[8] J. Zhang, C. You, H. Qi, C. Chen, X. Xu, Effect of solids concentration distribution on the flue gas desulfurization process., Environ. Sci. Technol. 40 (2006) 4010–5.

[9] M.J. Renedo, F. González, C. Pesquera, J. Fernández, Study of sorbents prepared from clays and CaO or $Ca(OH)_2$ for $SO_2$ removal at low temperature, Ind. Eng. Chem. Res. 45 (2006) 3752–3757.

[10] J.F. Sanders, T.C. Keener, J. Wang, Heated Fly Ash/Hydrated Lime Slurries for, 2 (1995) 302–307.

[11] H. Tsuchiai, T. Ishizuka, T. Ueno, H. Hattori, H. Kita, Highly active absorbent for $SO_2$ removal prepared from coal fly ash, Ind. Eng. Chem. Res. 34 (1995) 1404–1411..

[12] A. Al-Shawabkeh, H. Matsuda, M. Hasatani, Comparative reactivity of treated FBC- and PCC-fly ash for $SO_2$ removal, Can. J. Chem. Eng. 73 (1995) 678–685.

[13] J. Zhang, C. You, S. Zhao, C. Chen, H. Qi, Characteristics and reactivity of rapidly hydrated sorbent for semidry flue gas desulfurization., Environ. Sci. Technol. 42 (2008) 1705–1710.

[14] M.J. Renedo, J. Fernández, Preparation, characterization, and calcium utilization of fly Ash/$Ca(OH)_2$ sorbents for dry desulfurization at low temperature, Ind. Eng. Chem. Res. 41 (2002) 2412–2417.

[15] J. Fernández, M.J. Renedo, Study of the influence of calcium sulfate on fly ash/Ca(OH)2 sorbents for flue gas desulfurization, Energy and Fuels. 17 (2003) 1330–1337.

[16] M.J. Renedo, J. Fernández, Influence of different lignosulphonates on the properties of desulfurant sorbents prepared by hydration of Ca (OH)2 and fly ash, Ind. Eng. Chem. Res. 47 (2008) 1331–1335.

[17] P. Maina, M. Mbarawa, Use of fly ash, bottom ash and zeolite as additives for enhancing lime reactivity towards flue gas desulfurization, Environ. Prog. Sustain. Energy. 32 (2013) 75–83.

[18] A. Bueno-López, J. García-Martínez, A. García-García, A. Linares-Solano, Regenerable CaO sorbents for $SO_2$ retention: Carbonaceous versus inorganic dispersants, Fuel. 81 (2002) 2435–2438.

[19] G. Dube, P. Osifo, H. Rutto, Preparation of bagasse ash/MgO/ammonium acetate sorbent properties and modeling their desulphurization reaction, Environ. Prog. Sustain. Energy. 34 (2015) 23–31.

[20] R. del Valle-Zermeño, J. Giró-Paloma, J.Formosa, J.M. Chimenos, Low-Grade Magnesium Oxide by-products for environmental solutions: characterization and geochemical performance, J. Geochemical Explor. *In Press* (2014).

[21] R. del Valle-Zermeño, J.M. Chimenos, J. Formosa, A.I. Fernández, Hydration of a low-grade magnesium oxide. Lab-scale study, J. Chem. Technol. Biotechnol. 87 (2012) 1702–1708.

[22] M.A. Shand, The Chemistry and Technology of Magnesia, Wiley, 2006.

[23] C.A. Strydom, E.M. Van Der Merwe, M.E. Aphane, The effect of calcining conditions on the rehydration of dead burnt magnesium oxide using magnesium acetate as a hydrating agent, J. Therm. Anal. Calorim. 80 (2005) 659–662.

[24] H. Gao, C. Li, G. Zeng, W. Zhang, L. Shi, X. Fan, et al., Experimental study of wet flue gas desulphurization with a novel type PCF device, Chem. Eng. Process. Process Intensif. 50 (2011) 189–195.

[25] R. del Valle-Zermeño, J. Formosa, J.M. Chimenos, Wet Flue Gas Desulfurization: a Review, Rev. Chem. Eng *In Press* (2015).

[26] Y. Li, H. Qi, C. You, X. Xu, Kinetic model of CaO/fly ash sorbent for flue gas desulphurization at moderate temperatures, Fuel. 86 (2007) 785–792.

[27] M.J. Fernández, J., Renedo, Sulfation and Carbonation Competition in the Treatment of Flue gas from a Coal-Based Power Plant by Calcium Hydroxide, International Journal of Chemical Reactor Engineering. ISSN (Online) 1542-6580, ISSN (Print) 2194-5748, DOI: 10.1515/ijcre-2014-0182, January 2015.

[28] T. Nakazato, Y. Liu, K. Kato, Removal of SO2 in semi-dry flue gas desulfurization process with a powder-particle spouted bed, Can. J. Chem. Eng. 82 (2004) 110–115.

[29] G. Xu, Q. Guo, T. Kaneko, K. Kato, A new semi-dry desulfurization process using a powder-particle spouted bed, Adv. Environ. Res. 4 (2000) 9–18.

[30] J. Formosa, J.M. Chimenos, A.M. Lacasta, L. Haurie, Thermal study of low-grade magnesium hydroxide used as fire retardant and in passive fire protection, Thermochim. Acta. 515 (2011) 43–50.

[31] M. Josefina Renedo, C. Pesquera, F. González, J. Fernández, Use of TG-DSC-MS and gas analyzer data to investigate the reaction of $CO_2$ and $SO_2$ with $Ca(OH)_2$ at low temperature, Chem. Eng. Trans. 35 (2013) 739–744.